

# Indications of an Electronic Phase Transition in 2D $\text{YBa}_2\text{Cu}_3\text{O}_{7-x}$ Induced by Electrostatic Doping

Xiang Leng, Javier Garcia-Barriocanal, Boyi Yang, Yeonbae Lee, and A. M. Goldman  
*School of Physics and Astronomy, University of Minnesota, Minneapolis, Minnesota 55455, USA*  
(Dated: February 17, 2022)

We successfully tuned an underdoped ultrathin  $\text{YBa}_2\text{Cu}_3\text{O}_{7-x}$  film into the overdoped regime by means of electrostatic doping using an ionic liquid as a dielectric material. This process proved to be reversible. Transport measurements showed a series of anomalous features compared to chemically doped bulk samples and a different two-step doping mechanism for electrostatic doping was revealed. The normal resistance increased with carrier concentration on the overdoped side and the high temperature (180 K) Hall number peaked at a doping level of  $p \sim 0.15$ . These anomalous behaviors suggest that there is an electronic phase transition in the Fermi surface around the optimal doping level.

PACS numbers: 74.25.Dw, 74.25.F-, 74.40.Kb, 74.62.-c

The modulation of the electrical charge carrier density in strongly correlated electron systems using an electric field as an external control parameter is a long-standing goal in condensed matter physics due to its potential impact from both fundamental and technological points of view[1, 2]. Among those interesting materials, the application of field effect concepts to high temperature superconductors (HTSCs) is an active research field since it could provide a tool to control the density of the superconducting condensate in a reversible way, while keeping a fixed structure and avoiding changing the disorder associated with conventional doping by chemical substitution[3, 4]. Apart from potential applications, electrostatic doping of HTSCs is also a useful tool to study fundamental questions that still remain open such as the properties of the superconductor-insulator (SI) transition and the role of quantum criticality [5, 6].

Recently, the development of electronic double layer transistors (EDLT), that use ionic liquids (ILs) as gate dielectrics, has been successfully employed to achieve levels of doping of  $10^{15}/\text{cm}^2$ [7–9]. Taking advantage of such large charge transfers, this technique has been employed to successfully tune the SI transition in  $\text{La}_{2-x}\text{Sr}_x\text{CuO}_4$ (LSCO)[5] and in  $\text{YBa}_2\text{Cu}_3\text{O}_{7-x}$  (YBCO)[6], and to study the low carrier concentration side of the phase diagram. Both works reveal interesting physics on the nature of the quantum phase transition separating the superconducting and insulating phases when the density of charge carriers is depleted.

Nonetheless, the possibility of accumulating charge carriers by the field effect to tune an underdoped cuprate into the overdoped regime has remained elusive. For the 123 family of cuprate compounds, it has been shown that the  $\text{CuO}_2$  planes are only indirectly affected by the electric field since the injected holes are mainly induced in the  $\text{CuO}_x$  chains[10]. Moreover, the systematic preparation of YBCO bulk samples by tuning the oxygen stoichiometry in the overdoped region is difficult to achieve

and the highest level of overdoping is limited by the oxygen stoichiometric concentration, 0.194 holes/Cu for  $\text{YBa}_2\text{Cu}_3\text{O}_7$ [11].

Here we present a transport study of an electrostatically doped YBCO ultrathin film. We exploit the high local electric fields ( $10^9$  V/m) induced by an ionic liquid at the surface of the sample to tune the concentration of holes in the superconducting condensate across the top of the superconducting dome. The experiment reveals that the electrostatic doping of YBCO involves a different doping mechanism, as well as an anomalous normal resistance behavior in the overdoped regime. Surprisingly, we also find that the Hall number measured at 180 K displays a maximum around the optimal doping level that suggests the occurrence of an electronic phase transition separating the underdoped and overdoped regimes.

Ultrathin YBCO films were grown by means of a high pressure oxygen sputtering technique on (001) oriented  $\text{SrTiO}_3$  substrates. The technical details of sample preparation and characterization can be found in Ref. [6]. In order to determine the thickness threshold that separates insulating and superconducting samples, i.e. the thickness of the dead layer, we produced a series of thin films with thicknesses ranging from 5 to 10 unit cells. Using standard four-probe techniques we characterized the  $R(T)$  curves for each sample and we found that the 5-6 unit cells thick samples are insulating and the superconducting properties are completely recovered in a 7 unit cell thick film. The EDLT devices were fabricated using films of this thickness, following the procedure described in Ref. [8].

We monitored the gating process of the 7 unit cell YBCO ultrathin film by measuring the sheet resistance as a function of temperature(see Fig. 1). As can be seen in Fig. 1(a), the fresh sample, without any applied gate voltage ( $V_G$ ), has a transition temperature  $T_c = 42$  K. Here  $T_c$  was determined as the temperature corresponding to the crossing of the extrapolation of the fastest falling part of the  $R(T)$  curve to zero resistance. After

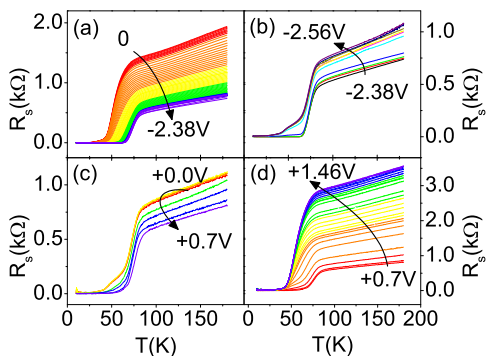


FIG. 1: (color online) Temperature dependence of the sheet resistance at different gate voltages. (a). From 0 to  $-1.2$  V,  $V_G$  was changed in  $-0.1$  V increments and then from  $-1.2$  to  $-2.38$  V, the increment was  $-0.02$  V. (b). From  $-2.38$  to  $-2.56$  V,  $V_G$  was changed in increments of  $-0.02$  V. (c). Negative  $V_G$  was then removed and a positive  $V_G$  was added. From 0 to  $0.7$  V,  $V_G$  was changed in  $0.1$  V increments. (d).  $V_G = 0.7, 0.75, 0.80, 0.85, 0.90, 0.95, 1.0, 1.05, 1.07, 1.10, 1.13, 1.15, 1.17, 1.20$  V, then the increment was changed to  $0.02$  V until  $V_G = 1.46$  V.

the application of a negative gate voltage,  $T_c$  increases and the normal state sheet resistance (the metallic region of the curve) drops. This is an indication that charge carriers are being injected into the sample and the concentration of holes is increasing towards the optimal doping point. For higher negative gating,  $V_G = -2.24$  to  $-2.38$  V, the rate of change of  $T_c$  and the normal resistance slows down and saturates.  $T_c$  reaches a maximum value of  $67$  K and the normal resistance reaches a minimum of  $750 \Omega$  at  $180$  K. We also observed small fluctuations in both  $T_c$  and the normal resistance in this regime. As shown in Fig. 1(b), upon a further increase of the negative gate voltage,  $T_c$  decreases, suggesting that the sample has been tuned into the overdoped regime. In addition, the normal resistance increases with increasing negative gate voltage, which is different from what is found in chemically doped bulk samples[12]. For the highest negative gate voltages ( $-2.46$  V  $< V_G < -2.56$  V) we note that the superconducting transition is not abrupt and a second transition is turned on at the lowest temperature part of the  $R(T)$  curve. We believe that this phenomenon is associated with the complete accumulation of holes in the top 1 to 2 unit cells which are the active layer of the sample, with the insulating dead layer underneath being affected by the high electric field.

To check the reversibility of the process and rule out a possible chemical reaction on the sample's surface we reversed the polarity of the gating. The result is shown in Fig. 1(c). After a threshold voltage of about  $+0.3$  V,  $T_c$  starts to increase and the normal resistance starts to drop, both of which are evidence of the recovery of optimal doping. With further increase in the positive

gate voltage, shown in Fig. 1(d),  $T_c$  drops and the normal resistance increases, revealing the complete recovery of the initial state of the sample and confirming that the electrostatic doping process is reversible.

In order to obtain an independent variable to describe the process of accumulation or depletion of holes we inferred an effective hole doping “p” by using the generic parabolic relation  $T_c/T_{c,\max} = 1 - 82.6(p - 0.16)^2$ [13]. We used this calculated number of holes to plot  $T_c$  and the values of normal resistance at  $180$  K (see Fig. 2). The open triangles represent the evolution of  $T_c$  and normal resistance at  $180$  K during the accumulation of holes, the depletion process is represented by the solid triangles. Interestingly, the normal resistance at  $180$  K exhibits a minimum around the optimal doping point, and its evolution with the number of holes per  $\text{CuO}_2$  plane roughly follows the same path in both the depletion and accumulation processes. This is a surprising behavior since in the overdoped region of the general bulk phase diagram of cuprates, the normal state is a Fermi liquid and a lowering of the normal resistance would be expected as the doping level increased. This raises the possibility that electrostatic doping is different from the chemical doping of bulk samples. Due to the short Thomas-Fermi screening length, the electric field affects only the surface layer (1 to 2 unit cells). Thus we are studying the properties of a 2D system whose physics might be different from that of bulk samples. Another possible effect, is the strong localization of the carriers resulting from the high local electric field induced by the accumulation of anions of the ionic liquid at the surface of the sample, or from the eventual increase of the electronic disorder at high levels of doping.

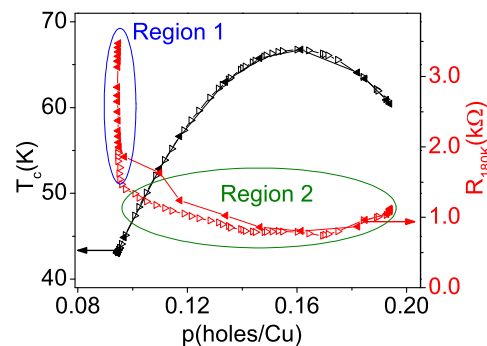


FIG. 2: (color online) Transition temperature ( $T_c$ ) and normal resistance at  $T=180$ K vs. effective hole doping,  $p$ . For both  $T_c$  and the normal resistance, data with negative values  $V_G$  are denoted by open triangles and data with positive  $V_G$ , by solid triangles.

Upon a closer inspection of Fig. 2, we notice that two different regions can be identified during the gating processes. The first one (region 1) shows an unchanged  $T_c$  over a large range of normal resistance change (i.e.

gate voltages) and it plays a primary role at the beginning and the end of the charging processes as holes are accumulated and depleted, respectively. The second region (region 2) is described above and it shows that the superconducting  $T_c$  and the normal resistance at 180 K are correlated and the superconducting properties of the sample are directly affected by the presence of the gate voltage. This is evidence that a threshold gate voltage is required for the doping of the superconducting planes. For gate voltages lower than the threshold,  $T_c$  is not affected and the doping process is manifested only by the changes of the normal resistance (region 1). Once the threshold is reached the superconducting properties are affected correspondingly (region 2).

Since the normal resistance is determined by the carriers both on the  $\text{CuO}_2$  planes and on the  $\text{CuO}_x$  chains while the superconducting property is mainly determined by the carriers on the  $\text{CuO}_2$  planes[14], our data suggest that the electrostatic doping of YBCO is actually a two-step process. First carriers are induced on the  $\text{CuO}_x$  chains and second, once a threshold concentration is reached, charge transfer occurs from the  $\text{CuO}_x$  chains to the  $\text{CuO}_2$  planes. In a previous study on  $\text{NdBa}_2\text{Cu}_3\text{O}_7$  in a backside gate configuration[10], Salluzzo *et al.* found that the holes injected by the electric field mainly dope the  $\text{CuO}_x$  chains while the  $\text{CuO}_2$  planes are only affected by the intra unit cell charge transfer from the  $\text{CuO}_x$  chains. Here we see that this charge transfer can happen only after a threshold carrier concentration on the  $\text{CuO}_x$  chains is reached and before this threshold, the electrostatic doping can affect only the  $\text{CuO}_x$  chains while the  $\text{CuO}_2$  planes are kept almost untouched. This two-step electrostatic doping process appears to be different from that of chemical doping, in which any changes of the hole doping in the range of  $0.05 < p < 0.2$  will affect the normal resistance and the superconducting properties simultaneously.

To develop insight into the nature of the anomalous normal resistance behavior in the overdoped region, we measured the Hall resistance at 180 K at different gate voltages. Figures 3(a) and 3(b) show the linear dependence of the transverse Hall resistance on magnetic field for different gate voltages. Hall resistances show a positive slope, which indicates that the charge carriers are holes as expected. In Fig. 3(c) the normalized Hall number as a function of hole concentration is shown. The Hall number is calculated from  $n_H = 1/(R_H e)$ , being  $R_H$  the Hall coefficient which is determined from the slope of the linear fit of the data plotted in Figs. 3(a) and 3(b). Interestingly, we find that the Hall number increases with the hole concentration up to  $p \sim 0.15$  whereupon an abrupt change takes place and a peak is developed.

The Hall effect of high- $T_c$  cuprates has been long studied and two scenarios have been proposed. One is the two relaxation time model[15, 16], in which the Hall relaxation rate  $1/\tau_H$  and the transport scattering rate  $1/\tau_{tr}$

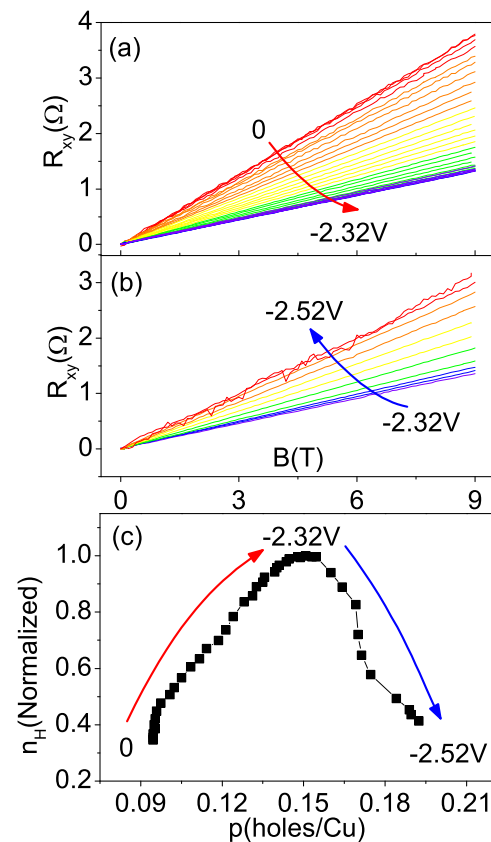


FIG. 3: (color online)(a) and (b), Hall resistance ( $R_{xy}$ ) vs. magnetic field at  $T=180\text{K}$  for different gate voltages. From 0 to  $-2.32\text{V}$ ,  $V_G$  changes  $-0.04\text{V}$  every time and from  $-2.32$  to  $-2.52\text{V}$   $V_G$  changes  $-0.02\text{V}$  every time. (c), Normalized Hall number ( $n_H$ ) vs. hole doping  $p$ .

are associate with spins and charges respectively. In the other scenario one has to consider the scattering from different regions of the Fermi surface[17]. Experimentally, anomalous dependence of the normal state Hall coefficient on the doping level has been reported in chemically doped YBCO[18],  $\text{Bi}_2\text{Sr}_{1.51}\text{La}_{0.49}\text{CuO}_{6+\delta}$  (BSLCO) [19] and LSCO[20]. In YBCO the Hall conductivity at 125 K showed anomalous behavior around the 60-K phase and in BSLCO and LSCO,  $n_H$  peaks around the optimal doping level at low temperature when superconductivity is suppressed by ultra high magnetic field. These anomalous behaviors are closely related to an unusual electronic state or a sudden change in the Fermi surface, although chemical doping might also change the magnetic coupling thus change the Hall scattering rate.

For electrostatic doping, it is hard to imagine that an electric field will change the magnetic coupling. Thus the  $n_H$  peak we observed indicates that there might be an electronic phase transition in the Fermi surface. Interestingly, in our results, the peak of the Hall number is found to be at  $p \sim 0.15$ , to the left of the optimal doping

point ( $p=0.16$ ). For a doping level of  $p=0.15$  the value expected for  $T^*$ , the pseudogap crossover temperature, roughly matches 180 K [21]. This would indicate that the electronic phase transition occurs at the boundary of the pseudogap state and the strange-metal state in the bulk phase diagram. However, the parabolic relation we used to derive the effective doping level might not be quantitatively right for a 2D film. Thus it is only safe to say the electronic phase transition we observed is around the optimal doping level, separating the underdoped regime and the overdoped regime.

Quantum oscillation experiments[14, 22–24] showed that while there is a large hole-like Fermi surface in the overdoped regime, there are only small pockets in the underdoped regime. Angle Resolved Photoemission Spectroscopy also showed that the transition from the overdoped to the underdoped regime is accompanied by an electronic reconstruction of the Fermi surface[25–29]. Thus an electronic phase transition in the Fermi surface is expected around the optimal doping regime. However, this anomalous behavior has never been widely reported in bulk samples and the similar peak observed in Ref. [19] disappeared at high temperature. This suggest that the electronic phase transition has been enhanced in our film, either due to the low dimensionality or the high local electric field.

In summary, we have studied the transport properties of an ultrathin YBCO film with the doping level changing from the underdoped regime to the overdoped regime by means of electrostatic doping. Our results reveal a two-step doping mechanism for the electrostatic doping of YBCO which is different from that of conventional chemical doping. Anomalous behavior of the normal resistance on the overdoped side was also accompanied by a peak in the high temperature (180 K) Hall number at  $p\sim 0.15$ . This suggests there is an electronic phase transition on the Fermi surface near the optimal doping point. The low dimensionality of the film or the high local electric field in the EDLT configuration might enhance this electronic phase transition and bring about these anomalous behaviors.

We would like to thank S. Bose and C. Leighton for their assistance with sample preparation and C. Geppert for his help with measurements. This work was supported by the National Science Foundation under grants NSF/DMR-0709584 and 0854752. Part of this work was

carried out at the University of Minnesota Characterization Facility, a member of the NSF-funded Materials Research Facilities Network via the MRSEC program, and the Nanofabrication Center which receives partial support from the NSF through the NNIN program. JGB thanks the Spanish Ministry of Education for the financial support through the National Program of Mobility of Human Resources (2008-2011).

- 
- [1] C. H. Ahn et al., *Rev. Mod. Phys.* **78**, 1185 (2006).
  - [2] C. H. Ahn et al., *Science* **284**, 1152 (1999).
  - [3] M. Imada, A. Fujimori, and Y. Tokura, *Rev. Mod. Phys.* **70**, 1039 (1998).
  - [4] J. Mannhart, *Superconductor Science and Technology* **9**, 49 (1996).
  - [5] A. T. Bollinger et al., *Nature* **472**, 458 (2011).
  - [6] X. Leng et al., *Phys. Rev. Lett.* **107**, 027001 (2011).
  - [7] J. T. Ye et al., *Nat Mater* **9**, 125 (2010).
  - [8] Y. Lee et al., *Phys. Rev. Lett.* **106**, 136809 (2011).
  - [9] H. Shimotani et al., *Applied Physics Letters* **91**, 082106 (2007).
  - [10] M. Salluzzo et al., *Phys. Rev. Lett.* **100**, 056810 (2008).
  - [11] R. Liang, D. A. Bonn, and W. N. Hardy, *Phys. Rev. B* **73**, 180505 (2006).
  - [12] S. H. Naqib et al., *Physica C* **387**, 365 (2003).
  - [13] J. L. Tallon et al., *Phys. Rev. B* **51**, 12911 (1995).
  - [14] N. Doiron-Leyraud et al., *Nature* **447**, 565 (2007).
  - [15] P. W. Anderson, *Phys. Rev. Lett.* **67**, 2092 (1991).
  - [16] T. R. Chien, Z. Z. Wang, and N. P. Ong, *Phys. Rev. Lett.* **67**, 2088 (1991).
  - [17] B. P. Stojković and D. Pines, *Phys. Rev. Lett.* **76**, 811 (1996).
  - [18] K. Segawa and Y. Ando, *Phys. Rev. Lett.* **86**, 4907 (2001).
  - [19] F. F. Balakirev et al., *Nature* **424**, 912 (2003).
  - [20] F. F. Balakirev et al., *Phys. Rev. Lett.* **102**, 017004 (2009).
  - [21] J. L. Tallon et al., *physica status solidi (b)* **215**, 531 (1999).
  - [22] C. Jaudet et al., *Phys. Rev. Lett.* **100**, 187005 (2008).
  - [23] B. Vignolle et al., *Nature* **455**, 952 (2008).
  - [24] D. LeBoeuf et al., *Nature* **450**, 533 (2007).
  - [25] M. R. Norman et al., *Nature* **392**, 157 (1998).
  - [26] K. M. Shen et al., *Science* **307**, 901 (2005).
  - [27] M. Platié et al., *Phys. Rev. Lett.* **95**, 077001 (2005).
  - [28] M. A. Hossain et al., *Nat Phys* **4**, 527 (2008).
  - [29] M. R. Norman, *Physics* **3**, 86 (2010).